Progress In Electromagnetics Research C, Vol. 34, 85–98, 2013

3.5/5 GHz DUAL-BAND 8 × 8 ADAPTIVE ARRAY ANTENNA

M. A. Soliman[1,*], T. E. Taha[2], W. Swelam[3], and A. Gomaa[4]

[1]National Telecom Regulatory Authority, Cairo, Egypt

[2]Faculty of Electronic Engineering, Menoufia University, Menouf, Egypt

[3]RF/Microwave and Photonics Group, Department of ECE, University of Waterloo, Ontario, Canada

[4]Shobraa Faculty of Engineering, Benha University, Cairo, Egypt

Abstract—In this paper, 4G smart planar dual-band phased array antenna suitable for fourth generation (4G) Long Term Evolution (LTE) at 3.5 GHz and also Wireless Local Area Network (WLAN) at 5 GHz systems is developed. The proposed planar array antenna is built using a microstrip rectangular U-slotted patch antenna element. Single element and linear sub-arrays with 1 × 2 and 1 × 4 dimensions of this element are designed, fabricated, and measured by the same authors. Separate feeding technique is used for each element of the smart planar array antenna; such that full beam-shaping can be achieved by steering the pattern main-loop to different angles in both azimuth and elevation directions with different amplitudes. Beam steering up to ±22 degrees can be achieved in both azimuth and elevation direction at 60 degree phase shift without the presence of any grating lobes. At this value of phase shift, the gain is 22.62 dBi without changing in the mutual coupling. This is also suitable for 4G Multiple-Input Multiple-Output (MIMO) wireless mobile applications with reduced power consumption. Design simulation and optimization processes are carried out with the aid of the Agilent Advanced Design System (ADS) electromagnetic simulator that uses the full-wave Method of Moment (MoM) numerical technique.

Received 15 August 2012, Accepted 22 October 2012, Scheduled 25 October 2012

* Corresponding author: Mohamed Ali Soliman (m_soliman23@hotmail.com).

1. INTRODUCTION

LTE is substantially improving end-user throughputs, sector capacity and reduce user plane latency to deliver a significantly improved user experience [1, 2]. It fulfills the requirements of International Mobile Telecommunications-Advanced (IMT-A): the group of the organization, International Telecommunications Union (ITU), interested in assigning the frequency bands of communications. As a result, this gives the requirements of the real 4G [3–6]. One of the frequency band needed for 4G is the band of 3.5 GHz [1, 4]. This band is useful also for Worldwide interoperability for Microwave Access (WiMAX) technology [3]. The frequency band of 5 GHz is suitable for Wireless Fidelity (Wi-Fi), the brand name of WLAN [3, 6]. Smart antenna can be helpful to achieve the requirements of WLAN and LTE 4G applications. Adaptive array antenna is used in such a way to reduce the interference, and hence enhance the signal to-noise ratio (SNR) [7–9]. All high throughput standards technologies (Wi-Fi, WiMAX, LTE, etc.) have adopted MIMO as part of the optional, if not mandatory portions of their standards [8]. As the number of the antennas increases in a MIMO system, less and less received power is needed to achieve the same date throughput rate [8]. At the same time, the use of MIMO systems increases the capacity of transferred signal as compared to the use of Single-Input Single-Output (SISO) and Single-Input Multiple-Output (SIMO) systems [10]. In this paper, we present 3.5/5 GHz dual-band 8×8 adaptive planar array antenna. The adaptation of the antenna is done by achieving different beam shaping. The proposed adaptive array antenna is built using a microstrip rectangular U-slotted patch antenna element. Single element and linear sub-arrays with 1×2 and 1×4 dimensions of this element were designed, fabricated and measured by the same authors [11, 12]. This paper is organized as follows.

Section 2 shows the developed array antenna design, simulation, and measurement for single element, 1×2, and 1×4 linear array antennas. Section 3 shows the 4×4 and 8×8 comparative studies. Section 4 shows the proposed smart array antenna and the examination of the accuracy and the efficiency of the simulation. Finally, Section 5 gives the conclusion.

2. SURVEY OF OUR PREVIOUS WORK

In this section, we show the developed array antenna design, simulation, and measurements for single element, 1×2, and 1×4 linear array antennas. We present the main mathematical equations that describe the MoM procedure.

2.1. Single Element Antenna

Figure 1 shows the geometry of an optimized antenna element (in mm). Rogers substrate, RT-Duroid 5880 ($\varepsilon_r = 2.2$). Single substrate is used with 62 mil thickness. U-shaped slotted patch is used to provide the dual-band for both the LTE and WLAN applications. A slot antenna has special advantages such as less conductor loss, wider bandwidth, and better isolation between the radiating element and fed network [13]. The effectiveness of dual-band slot antenna is confirmed and reported by [14–17], but for 2.4/5 GHz WLAN applications only. Our slot antenna is suitable for the both WLAN and WiMAX/LTE 4G applications. Design, simulation and optimization processes are carried out with the aid of ADS 2008 simulator which depends on MoM numerical technique [18]. MoM is one of the hardest to implement because it involves careful evaluation of Green's functions and EM coupling integrals. Maxwell's equations are transformed into integral equations which upon discretization yield the coupling matrix equation of the structure. The advantage of this transform is that the current distributions on the metal surfaces emerges as the core unknowns, this is in contrast to other techniques which typically have the electric and/or magnetic fields (present everywhere in the solution space) as the core unknowns. Hence, the number of unknowns (or the size of the matrix) is much smaller. This results in a very efficient simulation technique, which ia able to handle very complex structures [19]. The fundamental basics of MoM are best outlined as follows [20, 21].

To get into further details of the formulation, we start with the

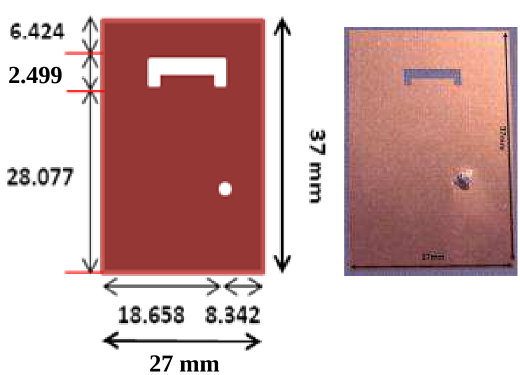

Figure 1. Geometry of a U-slotted antenna element.

conventional MoM procedure, whereby the mixed potential integral equation is discretized into a matrix equation:

$$\underline{\mathbf{Z}} \cdot \mathbf{I} = \mathbf{V}. \tag{1}$$

where $\underline{\mathbf{Z}}$ denotes the conventional MoM impedance matrix; $\mathbf{I}$ is the unknown current vector; and $\mathbf{V}$ is the excitation voltage vector. The desired solution $\mathbf{I}$ of (1) can be represented as:

$$\mathbf{I} = \sum_{i=1}^{N} \mathbf{c}_i \mathbf{I}_i, \tag{2}$$

where $\mathbf{I}_i$ $(i = 1, \ldots, N)$ represent the characteristic basis (CB) currents, and $\mathbf{c}_i$ denotes the "magnitudes" or weights of these currents.

We apply the Galerkin procedure once more and employ the Characteristic Basis (CB) as the testing functions.

This leads us to the following matrix equation for the "reduced current vector" $\mathbf{I}^R$ whose entries are the $\mathbf{c}_i$'s:

$$\underline{\mathbf{Z}}^R \cdot \mathbf{I}^R = \underline{\mathbf{B}}^T \cdot \mathbf{V} \tag{3}$$

Here $\underline{\mathbf{Z}}^R$ is an $N \times N$ reduced system matrix given by

$$\underline{\mathbf{Z}}^R = \underline{\mathbf{B}}^T \underline{\mathbf{Z}}^R \underline{\mathbf{B}}. \tag{4}$$

$\underline{\mathbf{B}}$ is a matrix with N columns defined by

$$\underline{\mathbf{B}} = [\mathbf{I}_1 \;\; \mathbf{I}_2 \;\; \ldots \;\; \mathbf{I}_N]. \tag{5}$$

The superscript "T" in the above equations denotes a matrix transpose. Several methods for fast matrix-vector multiplication that are available in the literature can be used to efficiently compute the coefficients in (3), if desired. As mentioned before, substituting the solution of Eq. (3) into the expression in Eq. (2) gives the induced current.

Antenna measurement is done using *hp*®8510C network analyzer.

Figure 2 shows that the reflection coefficient S_{11} for simulation is -23.83 dB at 3.5 GHz with a frequency bandwidth of 75 MHz

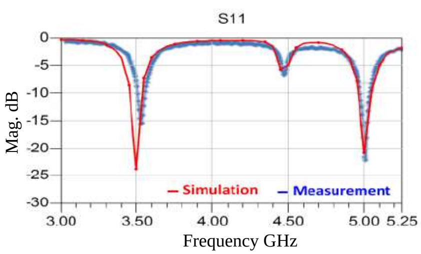

Figure 2. Single element reflection coefficient S_{11}.

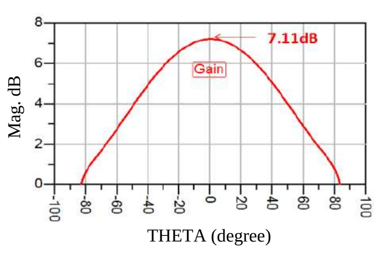

Figure 3. Single element gain.

(LTE frequency band), and is −20.88 dB with a frequency bandwidth of 80 MHz at 5 GHz (WLAN frequency band), respectively. S_{11} for measurement is −15.12 dB at 3.5 GHz and −21.22 dB at 5 GHz respectively. This ensures good matching between simulation and measurement. Figure 3 shows that the gain is better than 7 dBi with antenna efficiency of 93.43% at 3.5 GHz.

2.2. 1 × 2 Linear Array Antenna

Figure 4 shows the geometry of 1 × 2 array antenna element optimized in mm. Figure 5 shows that the reflection coefficients. S_{11} for simulation is −23.83 dB at 3.5 GHz and −20.01 at 5 GHz respectively. S_{22} for simulation is −20.88 dB at 3.5 GHz and −19.5 at 5 GHz respectively. S_{11} for measurement is −39.23 dB at 3.5 GHz and −18.73 dB at 5 GHz respectively and S_{22} for measurement is −35.82 dB at 3.5 GHz and −15.21 dB at 5 GHz respectively. This ensures good matching between simulation and measurement. Figure 6 shows the coupling coefficient S_{12}. This ensures good matching between simulation and measurement also.

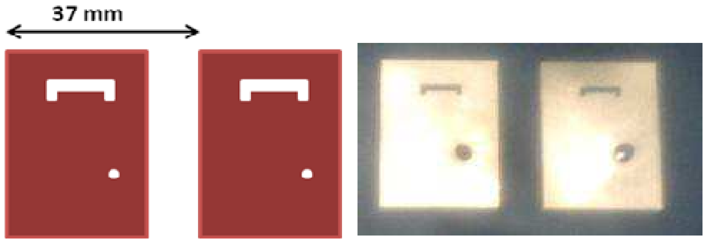

Figure 4. The 1 × 2 linear array antenna.

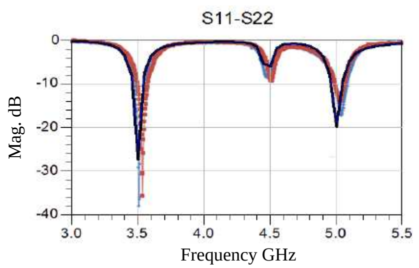

Figure 5. The 1 × 2 array reflection coefficients.

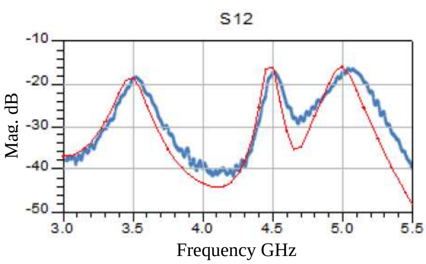

Figure 6. The 1 × 2 array coupling coefficients.

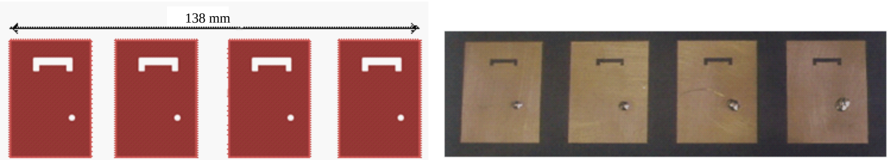

Figure 7. The 1×4 linear array antenna.

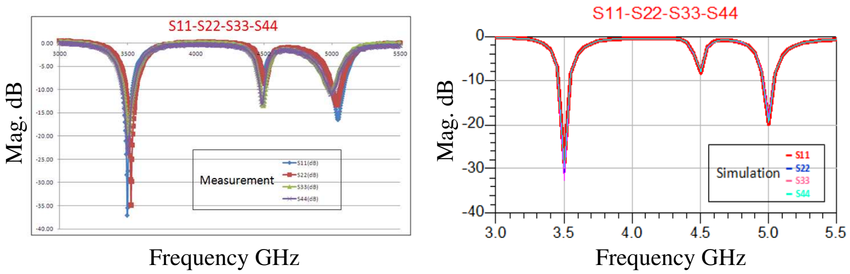

Figure 8. The 1×4 array reflection coefficients S_{11}, S_{22}, S_{33}, S_{44} for measurement and simulation.

2.3. 1×4 Linear Array Antenna

Figure 7 shows the geometry of 1×4 array antenna element optimized in mm. Figure 8 shows the reflection coefficients S_{11}, S_{22}, S_{33}, and S_{44}. This ensures good matching between simulation and measurement. Figure 9 shows the coupling coefficients S_{12}, S_{13} and S_{14}. This also ensures good matching between simulation and measurement.

Table 1 summarizes the antenna gain, efficiency, bandwidth, reflection coefficients, and coupling coefficients for single element, 1×2, and 1×4 linear array antennas at 3.5 GHz.

3. DISCUSSION OF THE COMPARATIVE PREVIOUS WORKS

In this section, we discuss and explain the previous studies related to the MIMO array antenna taking into consideration the design parameters, the frequency band used in the design, and the approach issue.

In [22], the optimum design for 4×4 planar Butler matrix array antenna was given for 5 GHz WLAN only. In that study, high dielectric constant was considered ($\varepsilon_r = 4.9$) and ($h = 1.6$ mm). Simulation was done by SONNET. In our previous work [23], compact 3.5/5 GHz

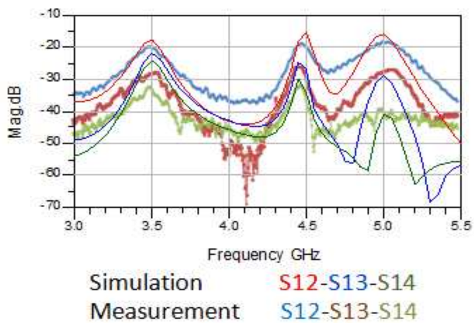

Figure 9. The 1×4 array coupling coefficients S_{12}, S_{13}, S_{14}.

Table 1. Gain, efficiency, bandwidth, reflection coefficients, and coupling coefficients.

	Gain	Efficiency	BW	Reflection Coefficients	Coupling Coefficients
Single element	7.441 dB	92.964%	78 MHz	−22.77 dB	—
1×2	9.528 dB	97.513%	80 MHz	−27.05 dB	−18.63 dB
1×4	12.329 dB	98.597%	81 MHz	−33.04 dB	Lies between −17.625 dB and −24.389 dB

dual-band planer 4×4 and 8×8 U-slotted rectangular patch array antennas were designed with dimensions of $137.9 \times 171.04\,\mathrm{mm}^2$ and $287 \times 367\,\mathrm{mm}^2$ respectively. The antennas were adaptively designed with beam steering at different angles. For 4×4 planer array antennas, beam steering up to ±62 degrees were achieved without any grating lobes at 3.5 GHz. Similarly, for 8×8 planer array antennas, beam steering up to ±78 degrees were achieved without any grating lobes at 3.5 GHz.

In [24], 4×4 adaptive elliptical array antenna was designed. The adaptation was done by changing the distance between elements in the array only. The approach dealt with fixed beams or those which were scanned by varying the frequencies. It was shown that the mutual coupling losses were increased when the element spacing decreased, but gain also was significantly decreased with it. The work of [24] is one of existing works in the literature.

Figure 10 shows the compact dual-band planar 4×4 U-slotted rectangular array antenna and Figure 11 shows the 4×4 planar array

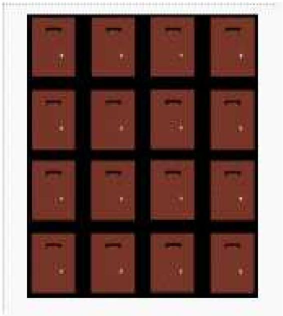

Figure 10. The compact dual-band planar 4 × 4 U-slotted rectangular patch array antenna.

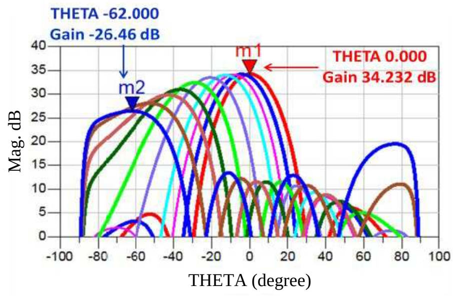

Figure 11. The 4 × 4 planar array beam steering.

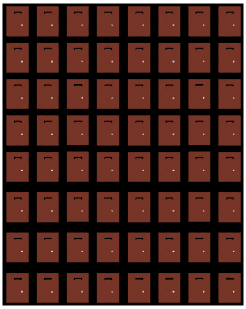

Figure 12. The compact dual-band planar 8 × 8 U-slotted rectangular patch array antenna.

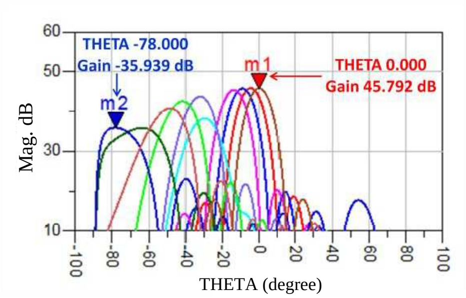

Figure 13. The 8 × 8 planar array beam steering.

beam steering. Similarly, Figure 12 shows the compact dual-band planar 8 × 8 U-slotted rectangular array antenna and Figure 13 shows the 8 × 8 planar array beam steering.

4. DESIGN OF OUR ADAPTIVE MODEL

In this section, we present our proposed smart array antenna explaining the idea of our approach. We examine the accuracy and efficiency of our simulation method by comparing it with another one.

The proposed 8 × 8 adaptive array antenna with the same dimensions of our previous work [23] is presented. The adaptation

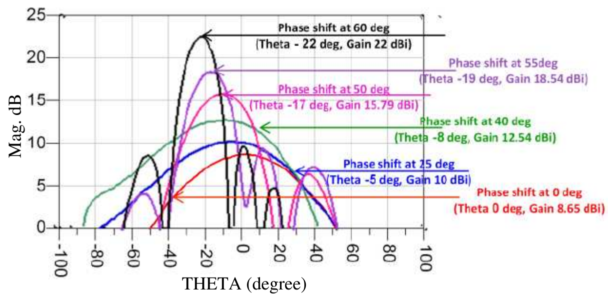

Figure 14. Gains with different steer angles at different phase shift angles.

Table 2. Phase shit difference, designated steer angle, and gain of 8×8 planar array antenna.

Phase shit difference ($\Delta\varphi$) [degree]	0	25	40	50	55	60
Designated steer angle (θ) [degree]	0	± 5	± 8	± 17	± 19	± 22
Gain [dBi]	8.65	10	12.54	15.79	18.54	22.62

is fulfilled by achieving different beam shaping. This is done by changing the feeding amplitudes distributions of the array element in both azimuth and elevation directions, and different feeding phase shift angles between different array elements in azimuth directions. This optimization method is the extension of [23], where the steering is performed by changing only phases of the elements feeding signals.

To examine the accuracy and efficiency of this smart antenna simulated by ADS using MoM technique, we compare it with the adaptive array antenna which was first used by [25] for Low Earth Orbit (LEO) satellite applications. For fair comparison, we use the same different amplitudes and phase shift angles changes which were done in [25]. Table 2 shows complete matching between both results, taking into consideration that the optimization process in [25] was done using a Genetic Algorithm (GA). Using a GA, gives very efficient optimization at exploring the entire space, but it is relatively poor in feeding the precise local optimal solution in region where the algorithm converges [26]. As a result, the validity of our simulation method is obtained, and at the same time it gets more efficient optimization process than GA process. GA process is one of the existing simulation methods that used extensively to deal with designing different types of antennas in the literature. Figure 14 shows the gain versus the designated steer angle for different phase shift differences. Table 2 shows the effectiveness of the proposed smart antenna by comparing it with the previous work [25] at 3.5 GHz as follows.

Table 3. The thinned elements at theta 0 deg.

<table>
<tr><th>ADS electromagnetic simulation result</th><th>GA result</th><th>Power distribution feeding With 0 phase shift</th></tr>
<tr><td>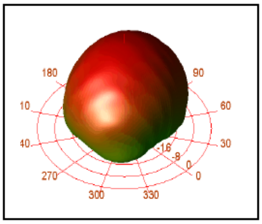</td><td>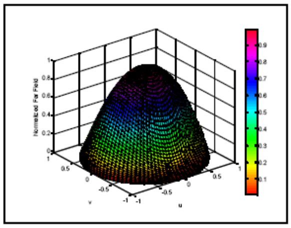</td><td>
<table>
<tr><td>1</td><td>1</td><td>0</td><td>0</td><td>0</td><td>0</td><td>0</td><td>0</td></tr>
<tr><td>0</td><td>0</td><td>0</td><td>0</td><td>0</td><td>0</td><td>0</td><td>0</td></tr>
<tr><td>0</td><td>0</td><td>0</td><td>0</td><td>0</td><td>0</td><td>0</td><td>0</td></tr>
<tr><td>0</td><td>0</td><td>0</td><td>0</td><td>0</td><td>0</td><td>0</td><td>0</td></tr>
<tr><td>0</td><td>0</td><td>0</td><td>0</td><td>0</td><td>0</td><td>0</td><td>0</td></tr>
<tr><td>0</td><td>0</td><td>0</td><td>0</td><td>0</td><td>0</td><td>0</td><td>0</td></tr>
<tr><td>0</td><td>0</td><td>0</td><td>0</td><td>0</td><td>0</td><td>0</td><td>0</td></tr>
<tr><td>0</td><td>0</td><td>0</td><td>0</td><td>0</td><td>0</td><td>0</td><td>0</td></tr>
</table>
</td></tr>
</table>

Table 4. The thinned elements at theta 25 deg.

<table>
<tr><th>ADS electromagnetic simulation result</th><th>GA result</th><th>Power distribution feeding With 25 deg phase shift</th></tr>
<tr><td>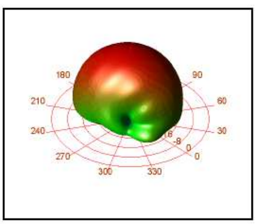</td><td>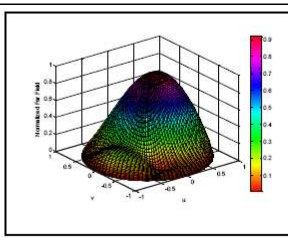</td><td>
<table>
<tr><td>1</td><td>0</td><td>0</td><td>0</td><td>0</td><td>0</td><td>0</td><td>0</td></tr>
<tr><td>1</td><td>1</td><td>0</td><td>0</td><td>0</td><td>0</td><td>0</td><td>0</td></tr>
<tr><td>0</td><td>0</td><td>0</td><td>0</td><td>0</td><td>0</td><td>0</td><td>0</td></tr>
<tr><td>0</td><td>0</td><td>0</td><td>0</td><td>0</td><td>0</td><td>0</td><td>0</td></tr>
<tr><td>0</td><td>0</td><td>0</td><td>0</td><td>0</td><td>0</td><td>0</td><td>0</td></tr>
<tr><td>0</td><td>0</td><td>0</td><td>0</td><td>0</td><td>0</td><td>0</td><td>0</td></tr>
<tr><td>0</td><td>0</td><td>0</td><td>0</td><td>0</td><td>0</td><td>0</td><td>0</td></tr>
<tr><td>0</td><td>0</td><td>0</td><td>0</td><td>0</td><td>0</td><td>0</td><td>0</td></tr>
</table>
</td></tr>
</table>

Table 5. The thinned elements at theta 40 deg.

<table>
<tr><th>ADS electromagnetic simulation result</th><th>GA result</th><th>Power distribution feeding With 40 deg phase shift</th></tr>
<tr><td>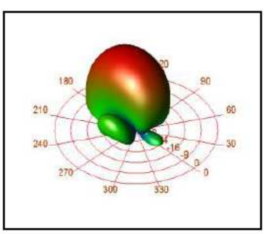</td><td>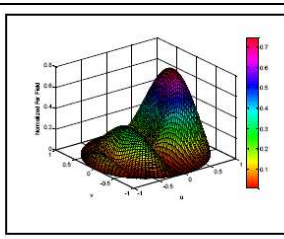</td><td>
<table>
<tr><td>1</td><td>1</td><td>0</td><td>0</td><td>0</td><td>0</td><td>0</td><td>0</td></tr>
<tr><td>1</td><td>1</td><td>0</td><td>0</td><td>0</td><td>0</td><td>0</td><td>0</td></tr>
<tr><td>1</td><td>1</td><td>0</td><td>0</td><td>0</td><td>0</td><td>0</td><td>0</td></tr>
<tr><td>0</td><td>0</td><td>0</td><td>0</td><td>0</td><td>0</td><td>0</td><td>0</td></tr>
<tr><td>0</td><td>0</td><td>0</td><td>0</td><td>0</td><td>0</td><td>0</td><td>0</td></tr>
<tr><td>0</td><td>0</td><td>0</td><td>0</td><td>0</td><td>0</td><td>0</td><td>0</td></tr>
<tr><td>0</td><td>0</td><td>0</td><td>0</td><td>0</td><td>0</td><td>0</td><td>0</td></tr>
<tr><td>0</td><td>0</td><td>0</td><td>0</td><td>0</td><td>0</td><td>0</td><td>0</td></tr>
</table>
</td></tr>
</table>

Table 6. The thinned elements at theta 50 deg.

ADS electromagnetic simulation result	GA result	Power distribution feeding With 50 deg phase shift
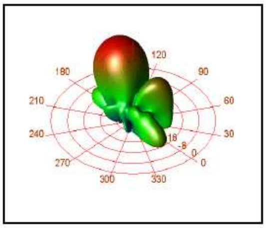	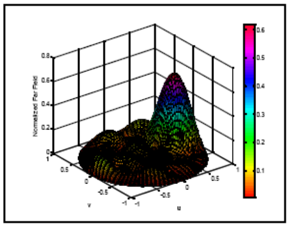	see grid below

1	0	1	0	0	0	0	0
1	1	1	1	0	0	0	0
1	1	1	1	0	0	0	0
1	1	0	1	0	0	0	0
0	0	0	0	0	0	0	0
0	0	0	0	0	0	0	0
0	0	0	0	0	0	0	0
0	0	0	0	0	0	0	0

Table 7. The thinned elements at theta 55 deg.

ADS electromagnetic simulation result	GA result	Power distribution feeding With 55 deg phase shift
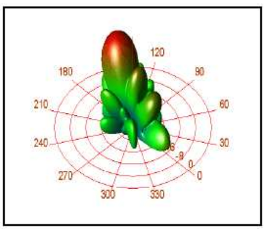	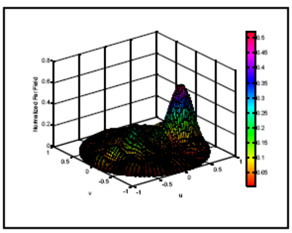	see grid below

1	1	0	1	1	1	0	0
1	0	1	0	1	1	0	0
1	1	1	1	1	1	0	0
1	0	1	1	1	1	0	0
1	0	1	1	1	1	0	0
0	0	0	0	0	0	0	0
0	0	0	0	0	0	0	0
0	0	0	0	0	0	0	0

Table 8. The thinned elements at theta 60 deg.

ADS electromagnetic simulation result	GA result	Power distribution feeding With 60 deg phase shift
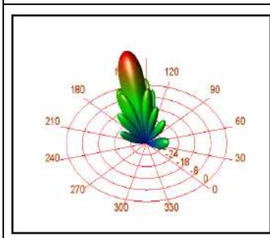	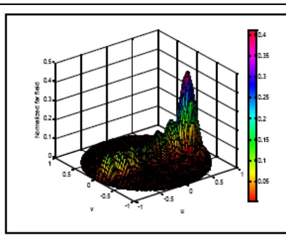	see grid below

1	1	1	1	1	1	1	1
1	1	1	1	1	1	1	1
1	1	1	1	1	1	1	1
1	1	1	1	1	1	1	1
1	1	1	1	1	1	1	1
1	1	1	1	1	1	1	1
1	1	1	1	1	1	1	1
1	1	1	1	1	1	1	1

The proposed smart planar array antenna with 8×8 dimensions will be used to achieve different beam shaping by changing the feeding amplitudes distribution of the array elements in both azimuth and elevation directions, and different feeding phase shift angles between different array elements in azimuth directions with values of 0, 25, 40, 50, 55 and 60 degrees. The electromagnetic simulation results will be verified with results of [25], using a GA. Tables 3, 4, 5, 6, 7, and 8 show complete matching between both results.

One of the interesting results is explained as follows: whatever the adaptation is done by changing the feeding amplitudes distributions or not, the mutual coupling does not changed, and lies between -14.022 and -58.141 dB for 8×8 array antennas without any grating lobes.

5. CONCLUSION

3.5/5 GHz dual-band 8×8 adaptive array antenna has been developed. This smart antenna is suitable for both MIMO LTE 4G and WLAN applications.

The previous comparative studies related to this work have been discussed. The theoretical fundamental of our simulator, ADS that uses MoM has been outlined. It has been shown that MoM is more efficient than GA method.

The adaptation of antenna has been done by changing the feeding amplitudes distributions of the array element in both azimuth and elevation directions, and different feeding phase shift angles between different array elements in azimuth direction.

The main interesting results are the saving in the gain of the antenna with different steering angles at different phase shifts without increasing the mutual coupling.

Numerically, it has been shown that beam steering of ± 22 degrees has been achieved at phase shift difference of 60 degree without any grating lobes at 3.5 GHz. The gain is saved with ranges between 8.65 and 22.62 dBi such that; the mutual coupling dos not changed and lies between -14.022 and -58.141 dB at different feeding phase shift angles, which lies between 0 and 60 degrees without any grating lobes.

REFERENCES

1. "Spectrum analysis for future LTE deployments," *Motorola White Paper*, 1–8, 2007.
2. Walsh, K. and J. Johnson, "3G/4G multimode cellular front end challenges, Part 1: Spectrum and regulatory issues," *RFMD White Paper*, No. WP09202, 2009.

3. Bourse, D. and R. Tafzolli, "Beyond 3G/4G ratio access technologies (RATs) and standards," *eMobility Tech. Platform White Paper*, Ver. 1, Dec. 2007.
4. "Transition to 4G: 3GPP broadband evolution to IMT-advanced 4G," Rysavy Research/3G Americas, Sep. 2010.
5. Rowinki, D., "Meet the real 4G," *ReadWrite Mobile*, Jan. 2012.
6. "Wireless tutorial: Wi-Fi, 3G, 4G, white space, and beyond," www.octoscope.com.
7. Jie, L. and Z. J. Wu, "The adaptive algorithm of the smart antenna system in 3G wireless communications systems," *Proceedings of the Int. Conf. on Signal Process.*, Beijing, China, Aug. 2002.
8. Daneshrod, B., "MIMO: The next revolution in wireless data communications," *Defense Electronics*, 57–59, Mar. 20, 2008, www.rfdesign.com.
9. Slyusar, V. I. and I. V. Titov, "Correction of smart antennas receiving channels characteristics for 4G mobile communications," *Proceedings of 4th Int. Conf. Antenna Theory and Techniques*, Sep. 2003.
10. Foschini, G. J., "Layered space-time architecture for wireless communication in a fading environment when using multi-element antennas," *Bell Labs Tech. Jour.*, 41–59, 1996.
11. Soliman, M. A., W. Swelam, A. Gomaa, and T. E. Taha, "Compact dual-band microstrip patch array antenna for MIMO 4G communication systems," *Proceeding of the IEEE Antennas & Propagation Symp.*, Toronto, Canada, Jul. 2010.
12. Soliman, M. A., W. Swelam, A. Gomaa, and T. E. Taha, "Compact dual-band microstrip patch array antenna for MIMO 4G LTE and WLAN systems," *Proceeding of 7th Int. Conf. on Electric. Eng.*, Cairo, Egypt, 2010.
13. Ysai, S. N., H. H. Hsin, H. K. Dai, and K. T. Chenge, "Accurate slot antenna assembly," US Patent No. 6373443, 2002.
14. Wu, J. W., "2.4/5 GHz dual-band triangular slot antenna with compact operation," *Microwave and Optical Tech. Lett.*, Vol. 45, 81–84, 2005.
15. Hsiao, H. M., J. W. Wu, and Y. D. Wang, "Novel dual-broadband rectangular-slot antenna for 2.4/5 GHz wireless communication," *Microwave and Optical Tech. Lett.*, Vol. 46, 197–201, 2005.
16. Ren, W., "Compact dual-band slot antenna for 2.4/5 GHz WLAN applications," *Progress In Electromagnetics Research B*, Vol. 8, 319–327, 2008.

17. Ali, J. K. and A. S. Emad, "A new fractal based printed slot antenna for dual-band wireless communication applications," *PIERS Proceedings*, 1518–1521, Kuala Lumpur, Malaysia, Mar. 27–30, 2012.
18. "Momentum software manual advanced design system," Agilent Technologies, Palo Alto, CA, 2008.
19. Van Hese, J., J. Sercu, D. Pissoort, and H. S. Lee, "State of the art in EM software for microwave engineers," *Agilent Technologies White Paper*, Feb. 2009.
20. Chen, R., K. Xu, and J. Ding, "Acceleration of MoM solver for scattering using graphics processing units (GPUs)," *Cross-strait Three Wireless Technology Seminar*, 63–66, Oriental Institute of Technology, Tapiei, Taiwan, 2008.
21. Mittra, R. and K. Du, "Characteristic basic function method for iteration-free solution of large method of moment problems," *Progress In Electromagnetics Research B*, Vol. 6, 307–336, 2008.
22. Bhowmik, W. and S. Srivastava, "Optimum design of a 4×4 planer Butler matrix array for WLAN application," *Jour. of Telcommun.*, Vol. 2, No. 1, 68–74, Apr. 2010.
23. Soliman, M. A., W. Swelam, A. Gomaa, and T. E. Taha, "Steerable dual-band planar microstrip phased array antenna for 3G and 4G wireless communication systems," *Proceeding of the IEEE Antennas & Propagation Symp.*, Toronto, Canada, Sep. 2011.
24. Madhav, B. T. P., K. Guru Pavani, M. Raveendra, and N. Revanth Teja, "Array antenna performance evaluation based on element spacing between the patches," *Int. Jour. of Emerging Tech. and Advanced Eng.*, Vol. 2, No. 3, 410–417, Mar. 2012.
25. El-Banna, H. H., A. A. Mitkees, A. M. Allam, and M. M. Mokhtar, "Antenna gain optimization for LEO satellites using a genetic algorithm," *Proceedings of 6th Int. Conf. on Electric. Eng.*, Cairo, Egypt, 2008.
26. Li, W. T., X. W. Shi, and L. Xu, "Improved GA and PSO called hybrid algorithm for antenna array pattern synthesis," *Progress In Electromagnetics Research*, Vol. 80, 461–476, 2008.